IMOS Integrated Marine Observing System

FACILITY 7: Australian Coastal Ocean Radar Network (ACORN)

Performance of the ACORN HF radar systems

Lucy R Wyatt
ACORN, School of Earth and Environmental Sciences,
James Cook University, QLD, 4811, Australia.
E-mail: lucy.wyatt@jcu.edu.au

February 2014

ACORN report 2014-1

JAMES COOK UNIVERSITY AUSTRALIA

TropWATER Centre for Tropical Water and Aquatic Ecosystem Research

Performance of the ACORN HF radar systems

Abstract

This is a study of the performance of the ACORN HF radars. It was originally motivated by a concern that the SeaSonde systems are not delivering the data quantity and quality that was expected of them but has developed into a review of the performance of all the radars. The analysis looks at the percentage return of radial and vector data as a function of range. The results show the variability in performance day and night, month by month and year by year at most sites due to a variety of factors. Periods of good performance can be identified and used as benchmarks by which to judge future performance.

1 Introduction

The Australian Coastal Ocean Radar Network (ACORN) is part of the Australian Integrated Marine Observing System (IMOS) which was set up with Australian Government funding in 2007. IMOS is designed to be a fully integrated national array of observing equipment to monitor the open oceans and coastal marine environment around Australia, covering physical, chemical and biological variables. All IMOS data is freely and openly available through the IMOS Ocean Portal for the benefit of Australian marine and climate science. The data management is carried out by the IMOS eMarine Information Infrastructure (eMII). HF radar provides maps of surface currents over meso-scale areas (typically up to 150km x 150km) of the coastal ocean. Deployment of the radars is in support of research into boundary currents and associated eddies, and their interaction with shelf water and topography. These physical phenomena are linked to productivity and connectivity of biological populations, and to management issues such as coral bleaching and disease transmission. The ACORN system provides a basis for applied research into wave modelling and offers test sites for hydrodynamic modelling.

ACORN currently operates 12 radars in 6 dual radar pairs at sites around the coast of Australia as shown in Fig. 1. The network includes 8 WERA [1] and 4 SeaSonde [2] radars. Four of the radar sites are in WA and four in SA of which half are WERAs and half SeaSondes. There are two WERA sites in NSW and two in QLD. WERAs have been used where there was a specific requirement for wave and wind, in addition to current, measurements. Although such measurements can be made with SeaSondes [3] they are confined to locations close to the radar sites. With phased array radars, of which WERA is an example, waves and winds can be mapped in a similar way to currents [4], albeit over a smaller area. The radar data are processed on site and files containing radial currents (current components along the radar beam directions) are transferred to the main ACORN server at James Cook University (JCU) where they are converted to netcdf files for deposition in the IMOS archive. Radial currents are combined to provide current vectors at JCU for the case of the SeaSonde data and by eMII for WERA data. All these data can be viewed and downloaded from the IMOS data portal http://imos.aodn.org.au/webportal/ normally in near real-time.

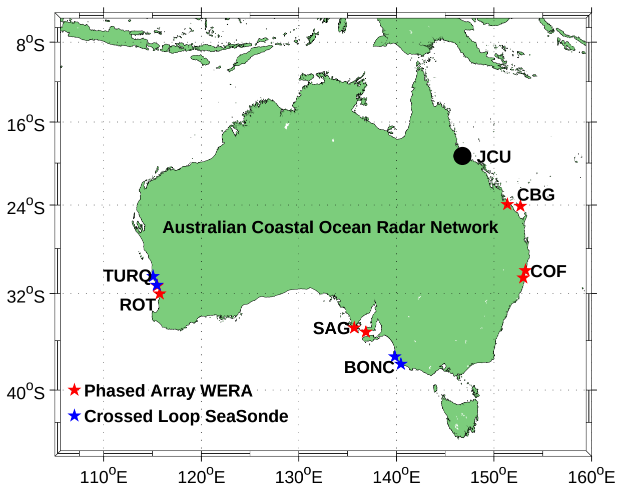

Figure 1: Map of Australia showing the ACORN radar locations.

ACORN is required to deliver files containing radial current data for at least 90% of the time. There is no specification on the quality of the delivered data although obviously it is ACORN's mission to ensure that the radars are operating correctly and delivering good data. In this report the data deliverable requirement is addressed and in addition the availability of radial and vector measurements as a function of range from the radars is addressed. This provides information both to judge the performance of existing radar systems and to provide guidance on potential performance at possible new sites.

2 Data Availability

ACORN has a target to deliver radar data from each station at least 90% of the time giving a potential radar data return for surface current measurement (which requires data from two radars) of about 81% assuming that interrruptions to data delivery from the two systems are independent. Table 1 shows the % of time that the radars delivered data files in 2011 to 2013. Note that the COF radars were only installed in 2012 and the TURQ radars were moved to the new locations during the period Dec 2012 to March 2013. The delivery of a radial data file indicates that the radars were running and the communication systems working. The vector data file statistics are derived from the monthly-aggregated hourly-averaged vector files. The numbers for the WERA systems are lower than expected probably because the vector files were generated (at eMII) before all the radial files had been uploaded. This has been the consequence of an ongoing communications issue between the JCU ACORN and eMII data servers which is slowly being resolved. The SeaSonde vector files are generated at JCU so have not suffered as much from this problem.

The figures do not give any information about the quality of the data in the files. This will be addressed in the next section. The figures show that, on average, ACORN is meeting the target for individual radar returns, with a small increase in performance in 2012, but that some stations and sites are below target. The main problems experienced in 2012 relate to loose cables; computer, hard drive, UPS and Tx amplifier failures; computers failing to reboot after a power outage. In some cases these indicate a lack of robustness of the radar hardware in the often difficult environmental conditions in which they operate. One case of vandalism also occurred. During 2011/12 automated monitoring procedures were significantly enhanced which will have contributed to the improved performance in 2012. However performance deteriorated slightly in 2013 possibly reflecting near end of lifetime for some system components.

3 Range performance

Range performance for individual radars has been measured by reading all the non-QC radial current files available on the IMOS server and calculating the % of time during each month when radial files exist for which there are radials in spatial bins of 10km by 20°. The median of these values for each range over the five direction bins between ±40° of boresight (as found in the radial files) has been used as the performance indicator. This analysis

Table 1: Radar data availability for 2011 to 2013

site	radar	station	2011		2012		2013	
			station	site	station	site	station	site
CBG	WERA	LEI	85.7	**69.4**	95.3	**68.9**	87.6	**62.1**
		TAN	98.1		95.9		94.1	
COF	WERA	RRK			98.9	**72.8**	96.1	**77.0**
		NNB			98.6		98.5	
BONC	SeaSonde	BFCV	96.5	**92.5**	95.6	**83.4**	96.4	**85.4**
		NOCR	95.9		95.2		95.0	
SAG	WERA	CSP	89.8	**72.0**	90.1	**68.4**	88.6	**88.1**
		CWI	87.6		99.5		99.4	
ROT	WERA	FRE	99.0	**83.6**	96.3	**74.7**	97.6	**87.6**
		GUI	93.8		96.9		90.2	
TURQ	SeaSonde	CRVT	93.9	**87.4**	88.9	**65.5**		
		SBRD	89.3		89.0			
TURQ	SeaSonde	GHED					99.0	**88.2**
		LANC					90.6	
		mean	93.0	**81.0**	95.0	**72.3**	94.4	**81.4**

has been carried out for the years 2010-2013. The monthly medians for each year and each radar are included in the Appendices. Annual averages of these monthly medians have been obtained and are shown here.

Figure 2 shows the results for the four SeaSonde radars. Note that in Dec 2012 the Cervantes (CRVT) radar was moved to Green Head (GHED) and in Apr 2013 the SeaBird (SBRD) radar was moved the Lancelin (LANC). The first of these moves was made (in part) to deal with the more limited performance of the radar at CRVT due to the siting of the Tx. Comparing the 2013 GHED performance with the previous performance of CRVT it can be seen that the system is achieving better range. The reduction in % annual data return at shorter ranges is due to problems during the first couple of months of this installation as is verified in Fig 3 which shows the monthly figures for this station. The SBRD station had to be moved further north to provide good dual radar coverage. The LANC site has suffered from severe erosion of the sand dunes which has necessitated two antenna moves each of which requires a new antenna pattern measurement. Some of the apparant reduction in performance of this system compared with its operations at

SBRD may be because the data on the IMOS portal have not yet all been updated with the latest calibrations. In general though performance of all the radars looks much better in 2013.

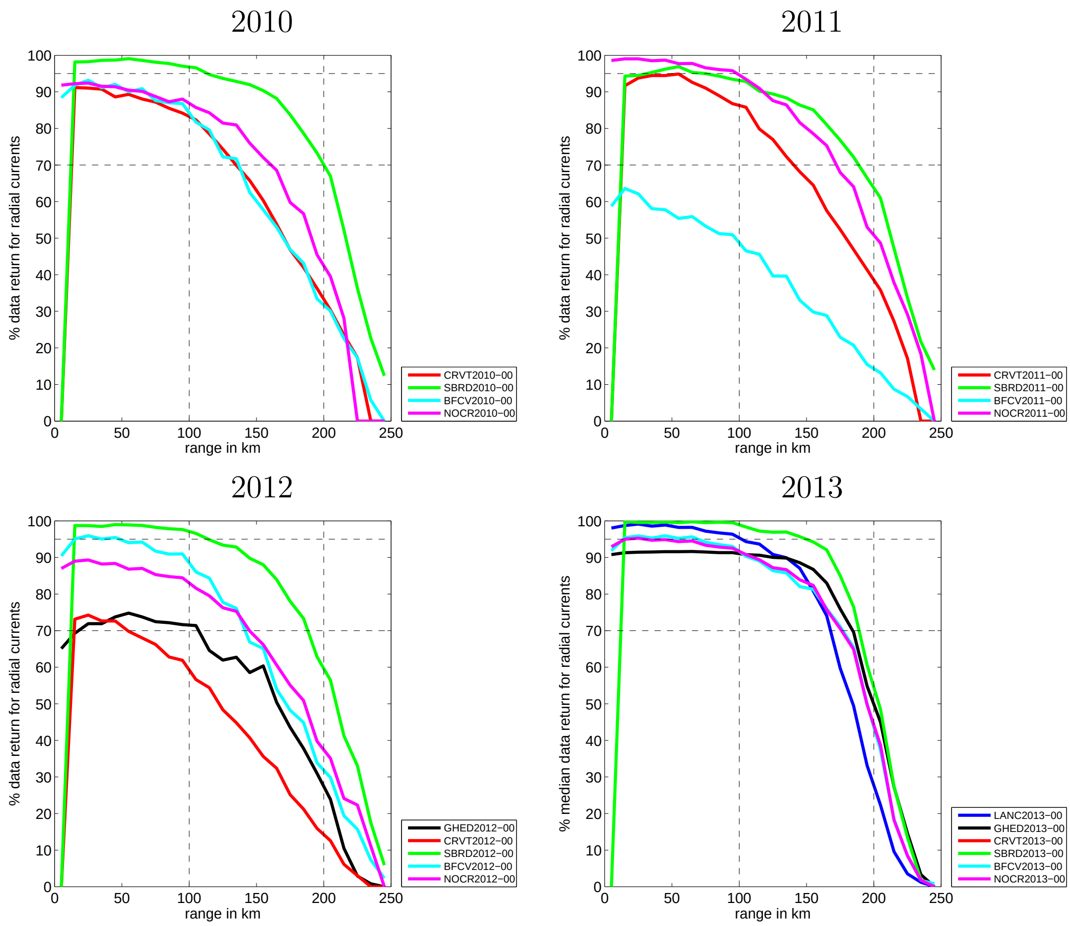

Figure 2: SeaSonde individual range performance

Figure 4 shows the results for the long range WERA systems and Figure 6 for the short range WERA systems. There appears to be a small deterioration in the long range WERA performance in 2013. The Cape Wiles (CWI) radar consistently outperforms the other systems and the annual figure remains high although the reduction in 2013 is reflecting a recent deterioration in the range acheived with this radar. The reason for this is not yet clear. The Guilderton (GUI) radar has also suffered a reduction in range during the latter half of 2013 due to an error in Tx cabling that has now been resolved. This is confirmed with the December figures shown in the 2013

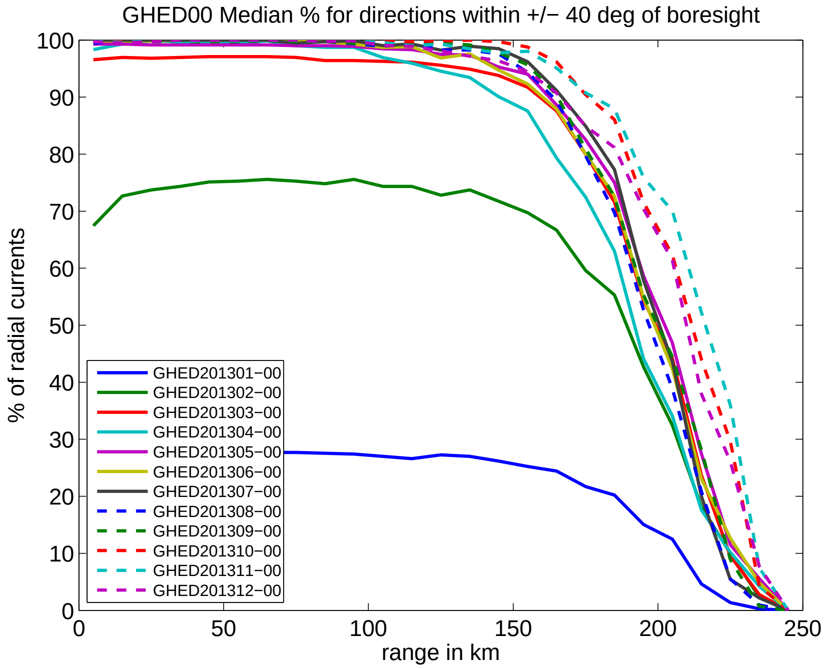

Figure 3: GHED 2013 range performance

monthly returns at this site in Fig 5. The Fremantle (FRE) radar has always been subject to more external noise limiting its range. All of these radar are showing signs of age and increased maintenance efforts are now required to get them back in shape. The Coffs Harbour radar range shown in Figure 6 is limited to 150km by the applied grid to keep the data files to a manageable size. The expected maximum range for these radars was 120km.

Of more importance for many oceanographic application is the coverage obtainable for vector currents. The figures for this have been obtained using all the monthly aggregated hourly-averaged (both non-QC and, in the case of WERA files, QC) vector current files on the IMOS server. For the SeaSonde cases these may not all have the latest calibration included which, when implemeted, may improve on the figures presented here. QC data are available for the WERA systems and although the radial analysis has not yet been done for these, the vector analysis has, and the two are compared here. Most of the vector analysis though is limited to the non-QC data. The data have again been binned into range-azimuth bins using the maximum range and maximum azimuth of the two radars contributing to the measurement at each location. The shortest range will depend on the configuration of the two radars, in particular on their separation and on the angle between their

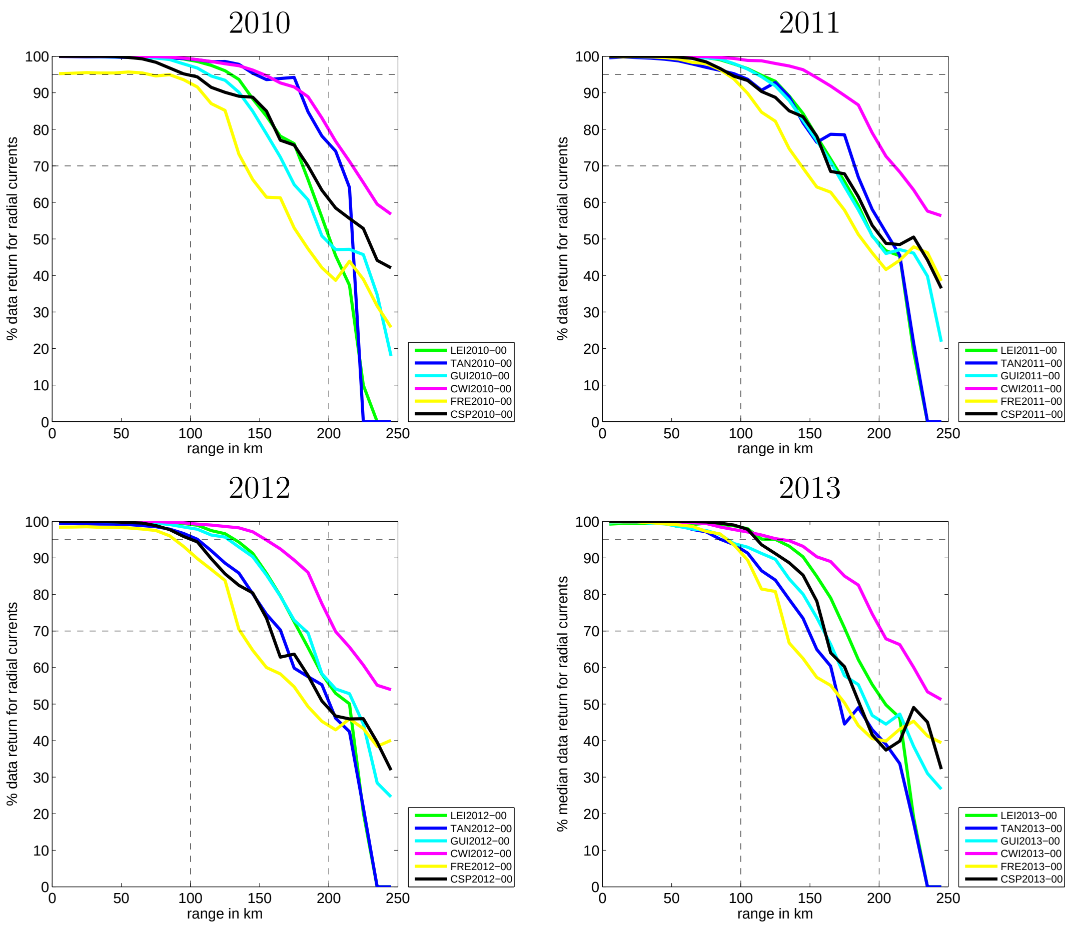

Figure 4: Long range WERA individual range performance

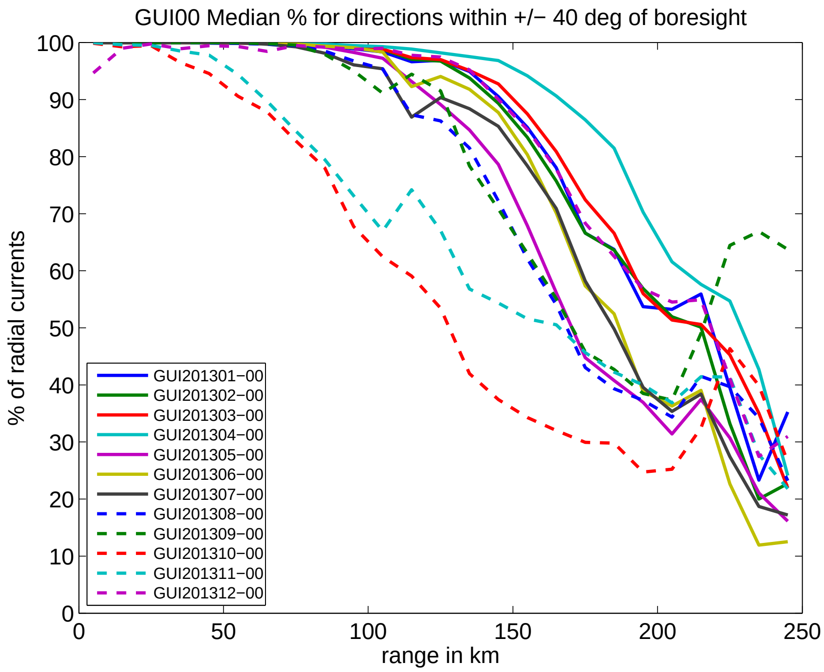

Figure 5: GUI 2013 range performance

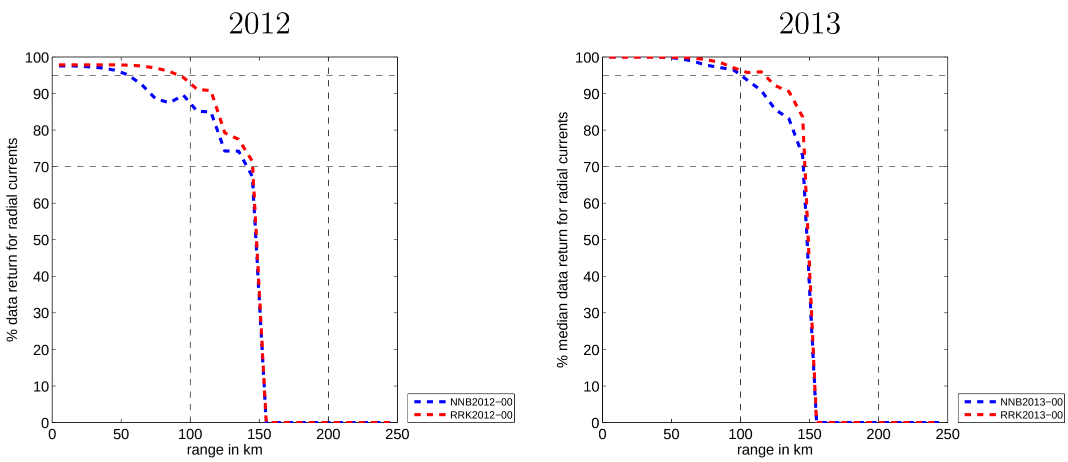

Figure 6: Medium range WERA individual range performance

boresights (see Table 2) although the latter is less of an issue for the SeaSonde radars since they are broad beam. Two performance indicators have been calculated, the maximum and median % returns across all azimuths in a given range bin. Here the % is measured relative to the total number of hours in a month for which an hourly averaged data set is included in the monthly aggregated file.

Figure 7 shows the results for the two SeaSonde radar sites. The absence of data at short ranges is because the maximum of the two ranges has been used and the radars are separated by about 100km (see Table 2. The angle between the two boresights probably explains why the minimum range for the newer TURQ configuration is less that that of the older even though the distance between the sites is greater. Figure 8 shows the corresponding results for the long range WERA systems and Figure 9 for the short range WERA systems. Here it can be seen that, although the ranges acheived for radial data are similar to those of the SeaSonde the vector coverage is more limited in range with the WERA. This is most likely due to the limited azimuthal coverage of WERA. This contrast between radial and vector range for SeaSonde and WERA can be seen more clearly in Figure 10 which shows the radial and vector % returns for each dual radar site in 2013. The radial covereage for SeaSonde radars seems to give a much better indicator of potential vector coverage than is the case for WERA. Note though that the figures are not directly comparable. They are percentages of the data in data files on the IMOS server and gaps may still exist there. The COF figure in Figure 10 shows that the 150km limit that was placed on the grid and which seemed a bit short based on the radial percentages, is more than enough for the vectors.

The non-QC and QC data comparisons for 2010-2013 are in the Appendices for each WERA system. It is clear that the QC data has consistently higher data returns. The figures for 2013 are also shown in Fig 11 below.

References

[1] Gurgel K.-W., G. Antonischki, H-H. Essen and T. Schlick, "Wellen Radar (WERA): a new ground-wave HF radar for ocean remote sensing", *Coastal Engineering*, 1999, 37, 219-234.

[2] Lipa, B.J., B. Nyden, D. Ullman, E. Terrill, "SeaSonde radial velocities: derivation and internal consistency", *IEEE Journal of Oceanic Engineering*, October 2006, vol.31, no. 4, pp. 850- 861.

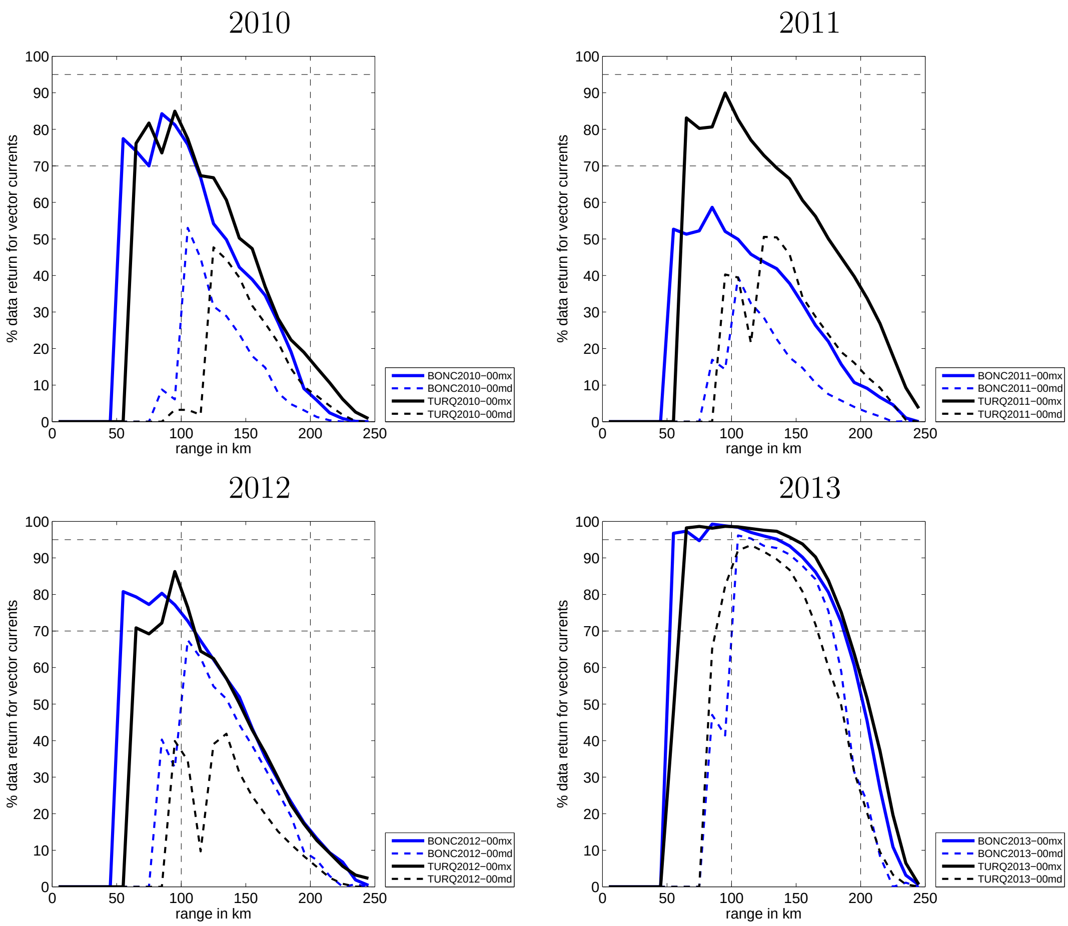

Figure 7: SeaSonde vector range performance

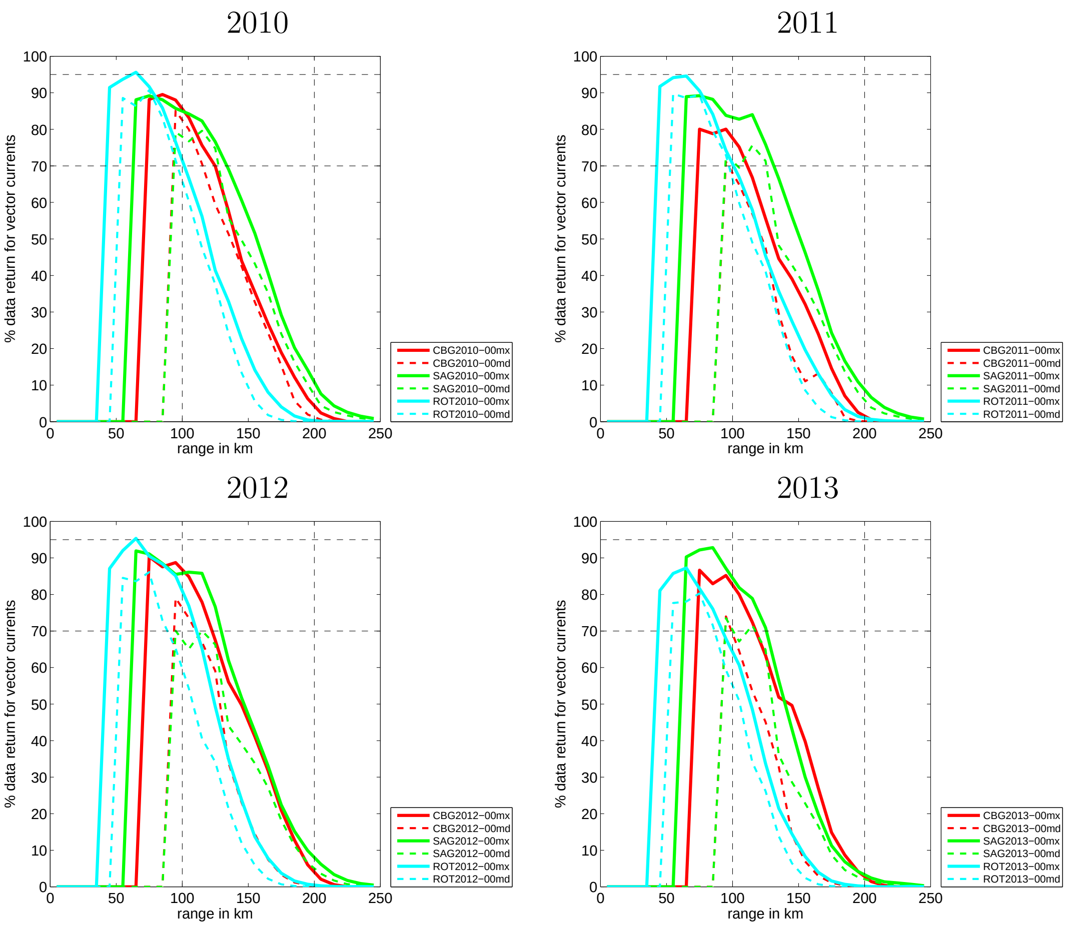

Figure 8: Long range WERA vector range performance

Table 2: Radar configuration factors influencing vector data return

site	radar	distance	boresights	angle
BONC	SeaSonde	86	255/257	2
TURQ 2010-12	SeaSonde	94	278/288	10
TURQ 2013	SeaSonde	112	290/235	55
CBG	WERA	138	45/317	88
SAG	WERA	116	189/243	54
ROT	WERA	80	285/230	55
COF	WERA	74	132/68	64

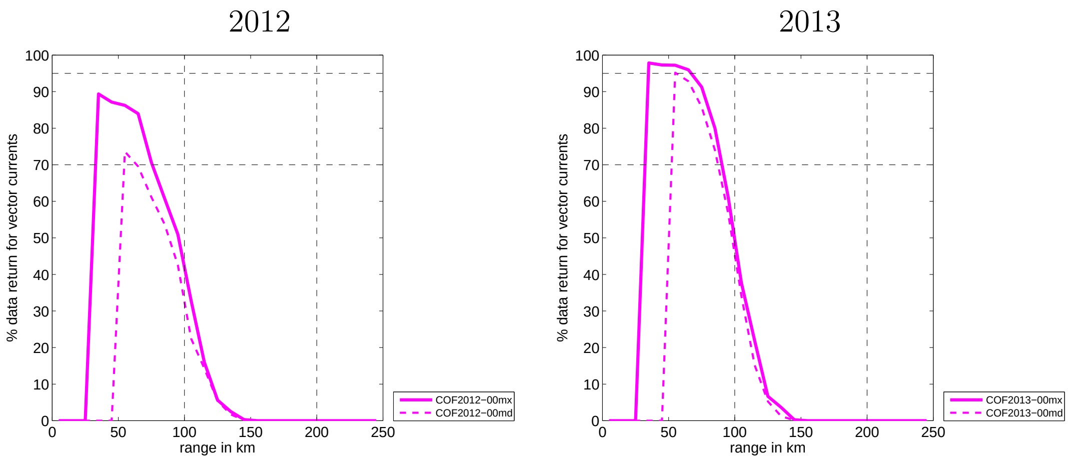

Figure 9: Medium range WERA vector range performance

[3] Lipa B. and B. Nyden. “Directional wave information from the SeaSonde”, *IEEE Journal of Oceanic Engineering*, 2005, 30, 221-231.

[4] Wyatt L.R., J.J. Green, K-W. Gurgel , J.C. Nieto Borge , K. Reichert , K. Hessner, H. Gnther, W. Rosenthal, . Saetra and M. Reistad,.”Validation and intercomparisons of wave measurements and models during the EuroROSE experiments”, *Coastal Engineering*, 2003, 48, 1-28.

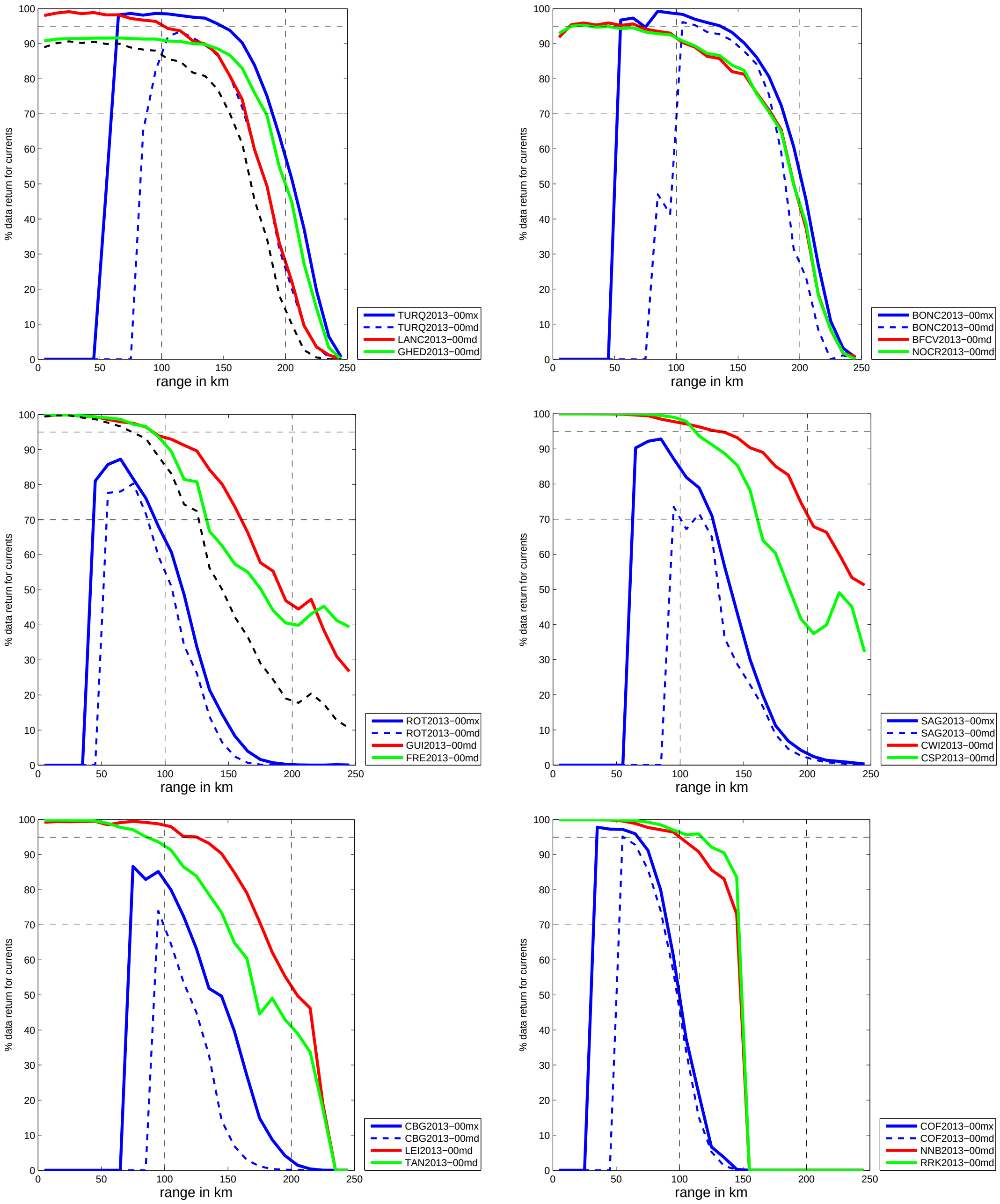

Figure 10: Radial and vector range performance

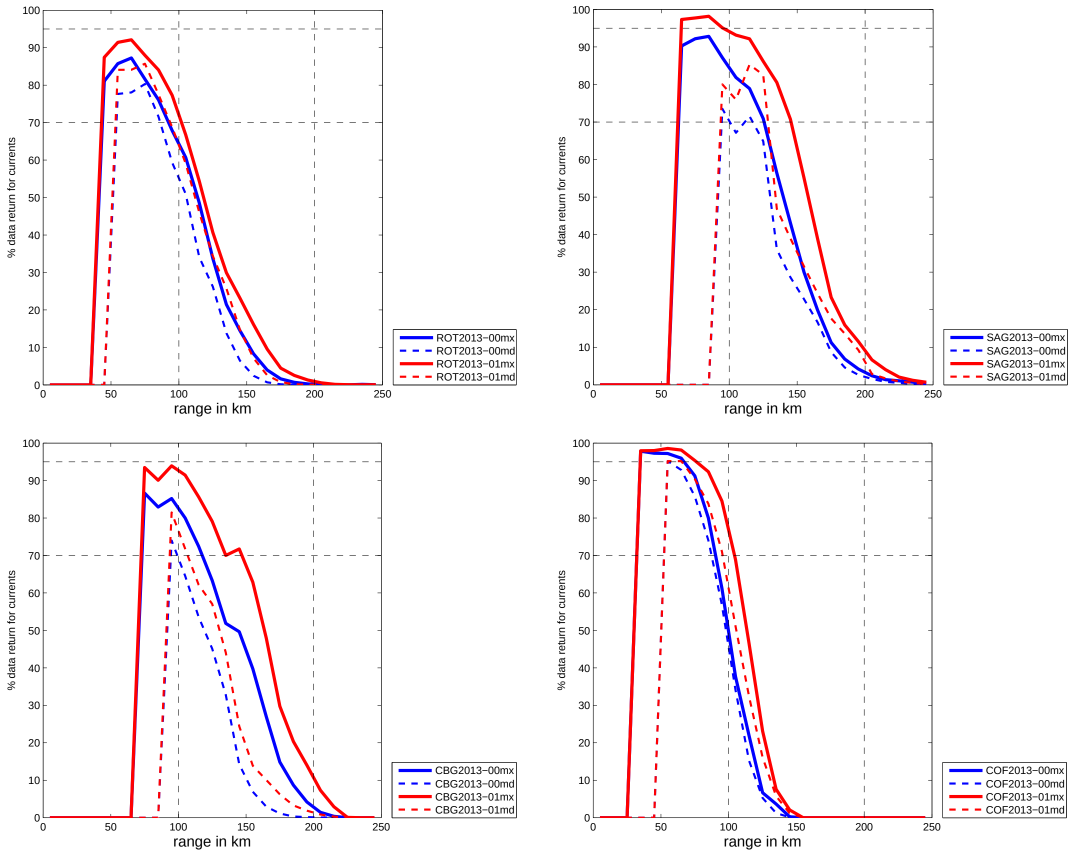

Figure 11: Non-QC (blue) and QC WERA vector data return for 2013.

Appendix 1: Performance of the CBG radars

In first section of this appendix the monthly performance of the CBG radar is presented. The second section shows the annual vector returns showing the average diurnal variation due to different ionospheric conditions. The third section shows the yearly-average comparison between QC and non-QC data.

4 Monthly Returns

Figure 12 shows the 50 and 90% data return ranges for each radar for the period of the deployment. Gaps in the data (connected with strainght lines in this figure) could mean there were no data or that the data are not on the IMOS server. Figure 13 and Figure 14 show the monthly returns for each radar for each year.

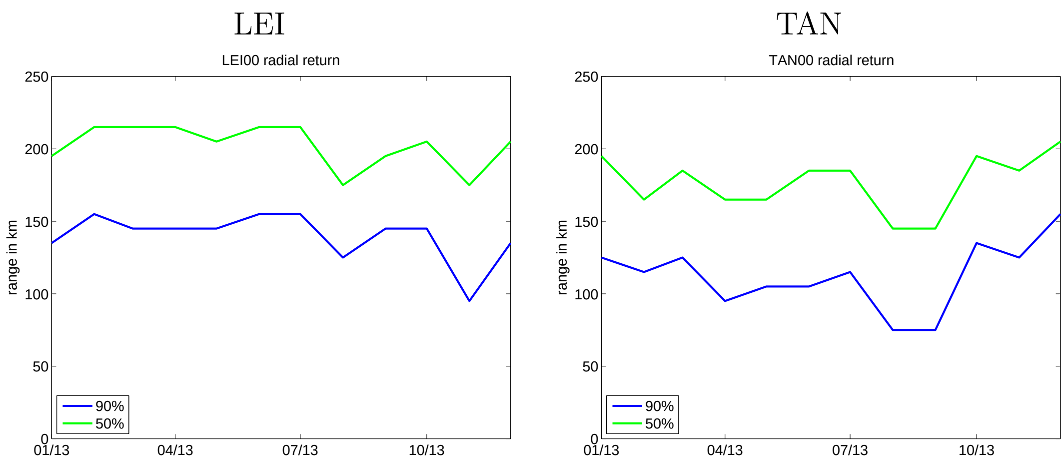

Figure 12: 50 and 90 percent data return ranges

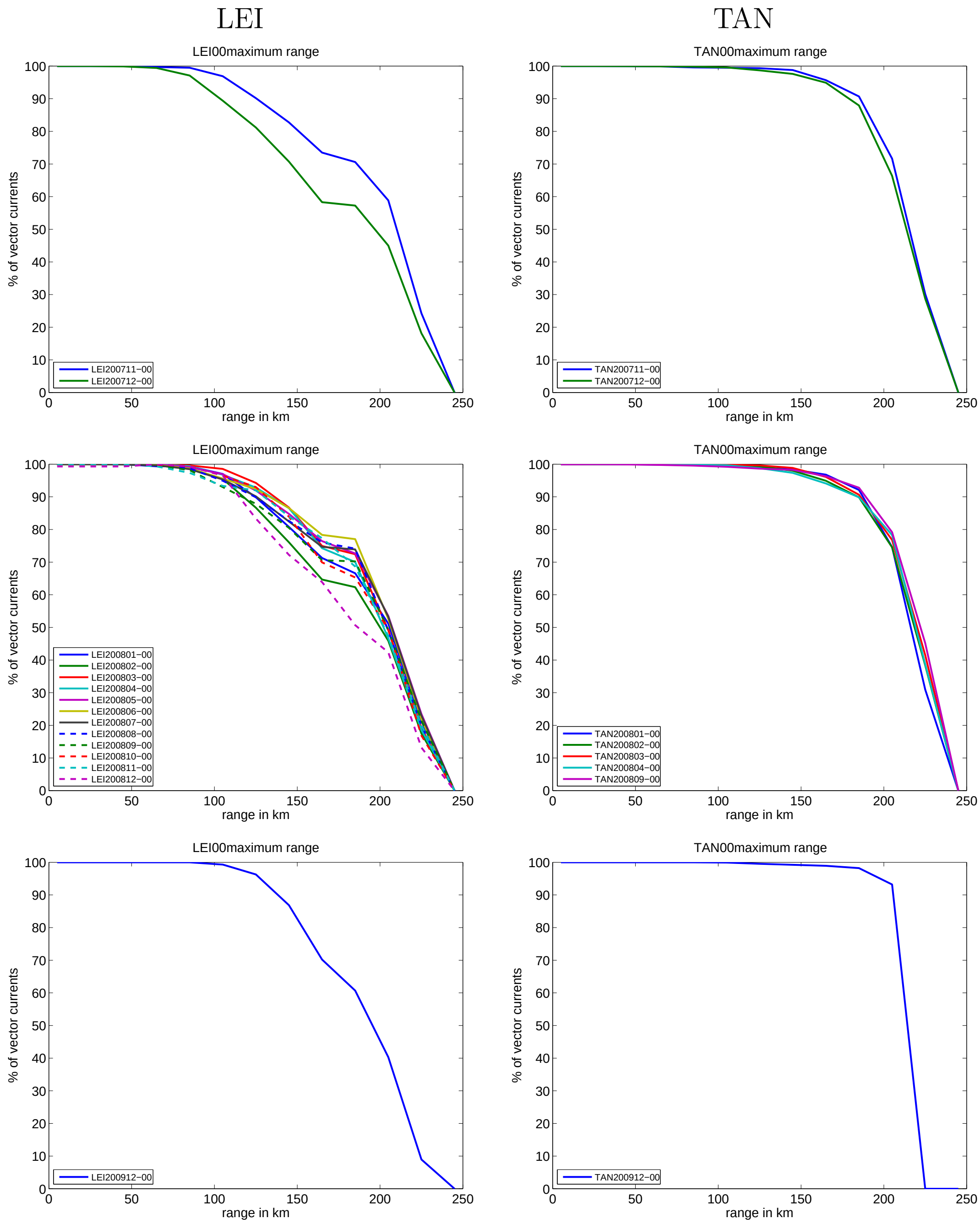

Figure 13: Radial % data return ranges 2007-2009

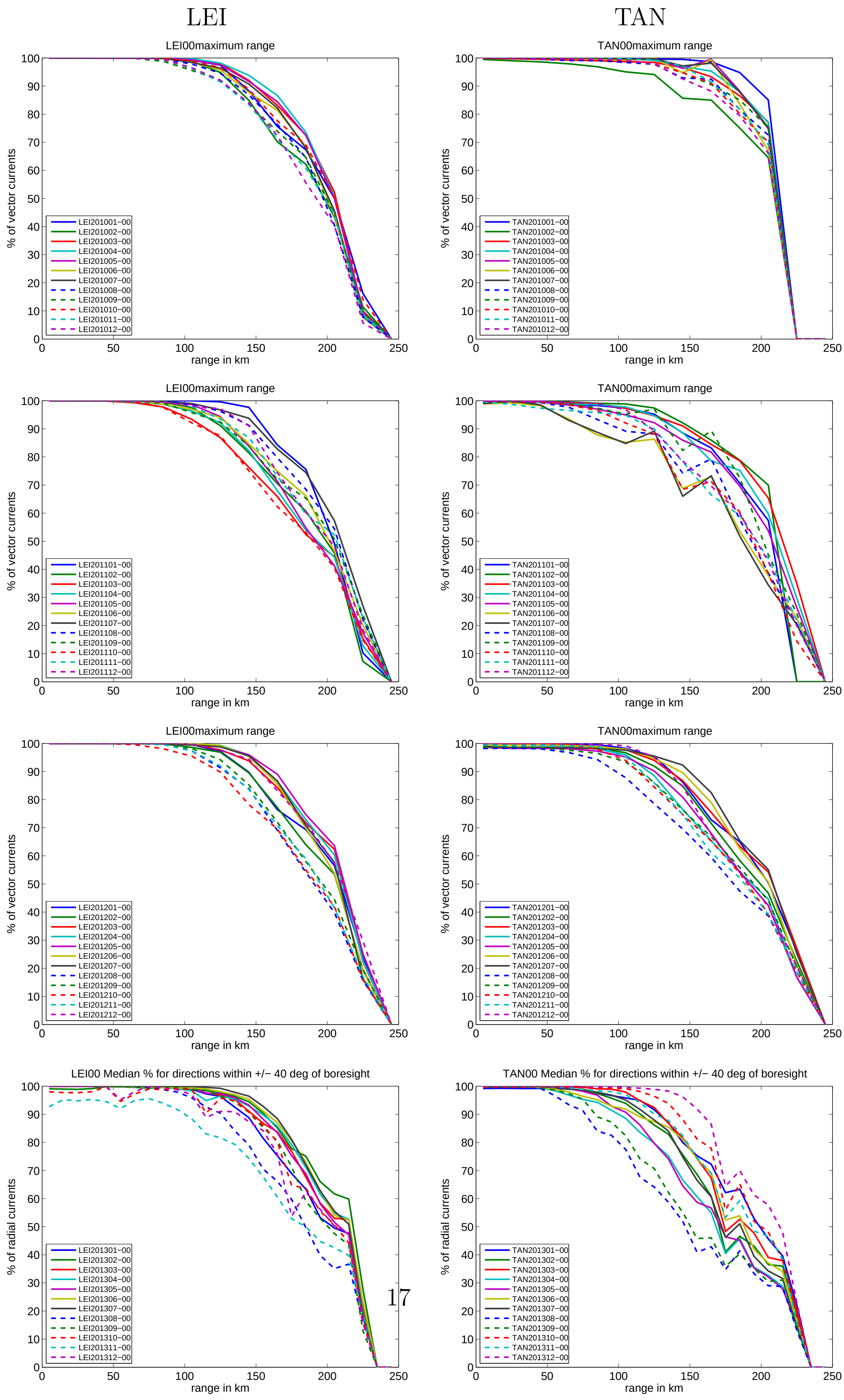

Figure 14: Radial % data return ranges 2010-2013

5 Annual mean Day-Night Returns

Figure 15 shows the median percentage vector data return for this site together with the % return broken down by time of day to show the impact of the ionosphere.

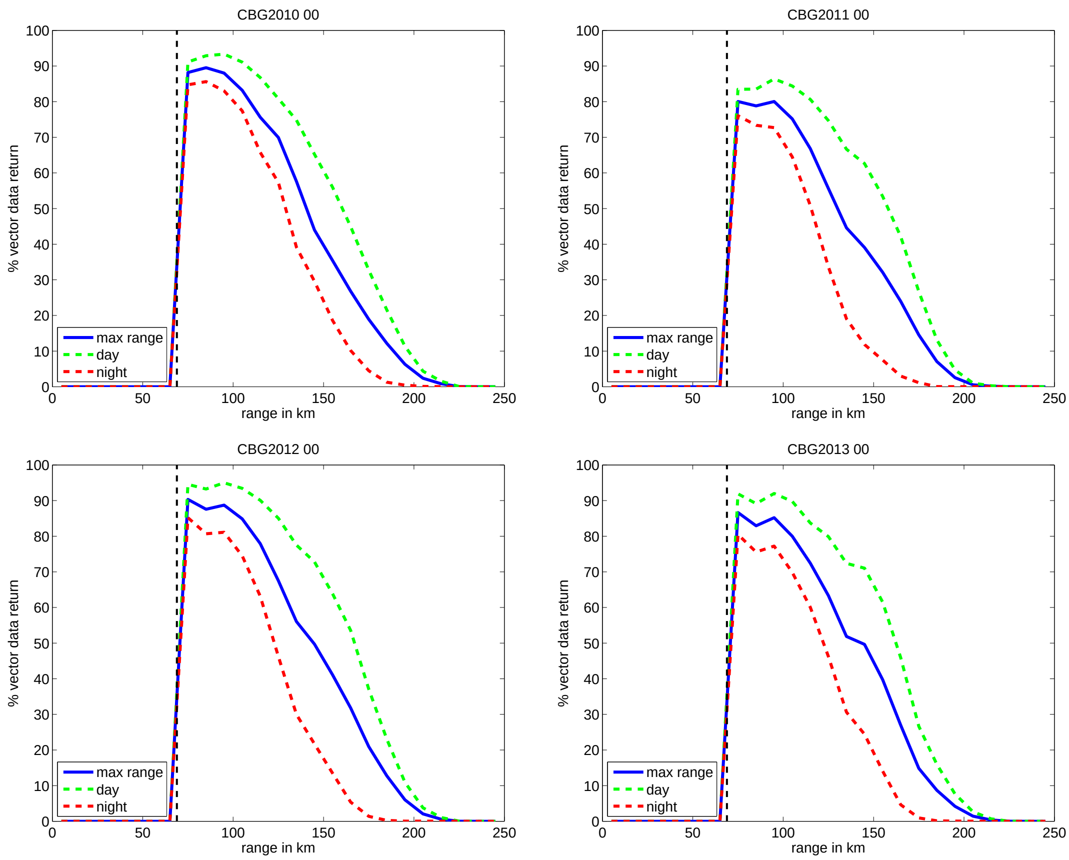

Figure 15: Vector % data return ranges 2010-2013

6 Annual mean QC and non-QC Returns

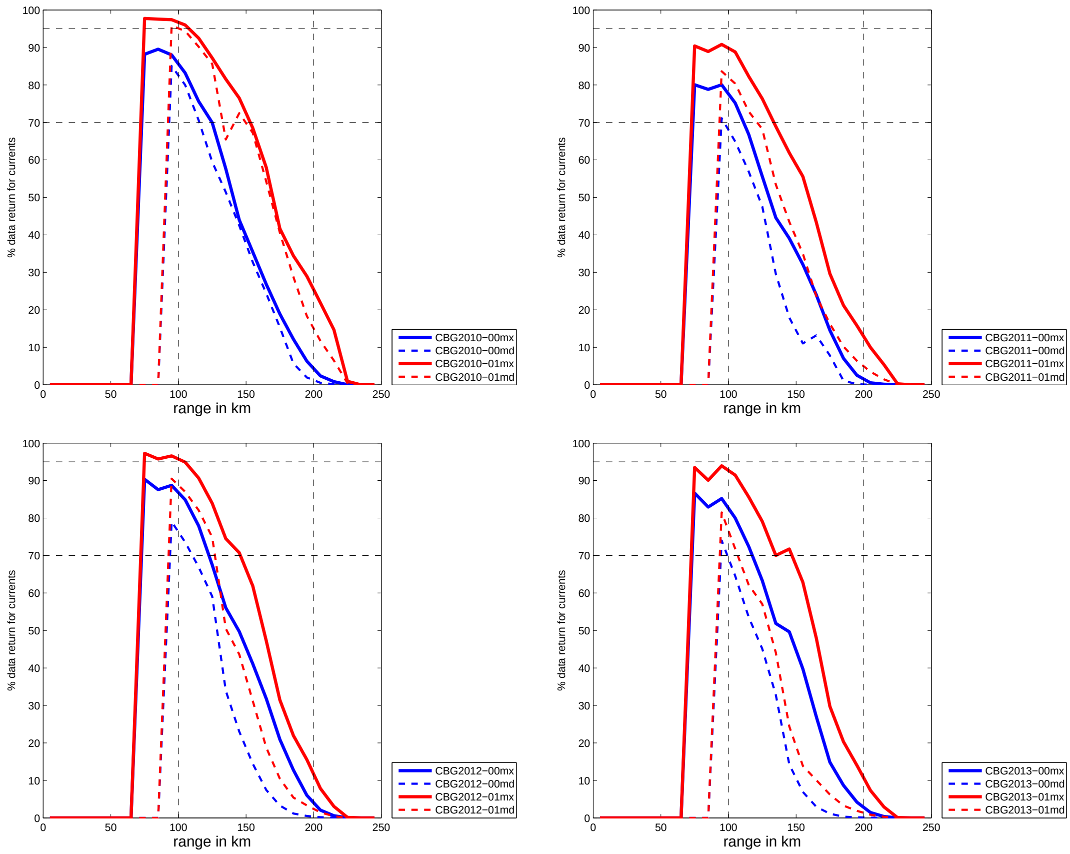

Figure 16: Comparison of QC and non-QC vector % data return ranges 2010-2013

Appendix 2: Performance of the COF radars

In first section of this appendix the monthly performance of the COF radar is presented. The second section shows the annual vector returns showing the average diurnal variation due to different ionospheric conditions. The third section shows the yearly-average comparison between QC and non-QC data.

7 Monthly Returns

Figure 17 shows the 50 and 90% data return ranges for each radar for the period of the deployment. Gaps in the data (connected with strainght lines in this figure) could mean there were no data or that the data are not on the IMOS server. Figure 18 show the monthly returns for each radar for each year.

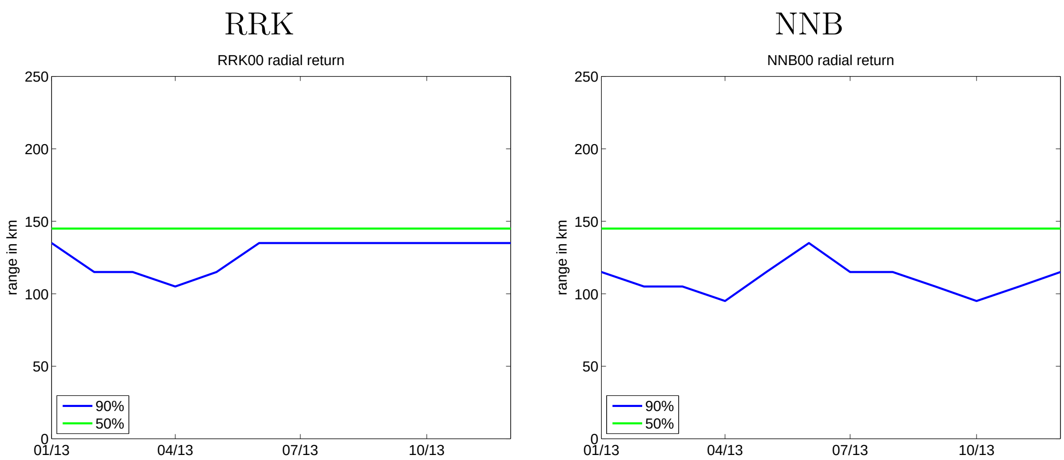

Figure 17: 50 and 90 percent data return ranges

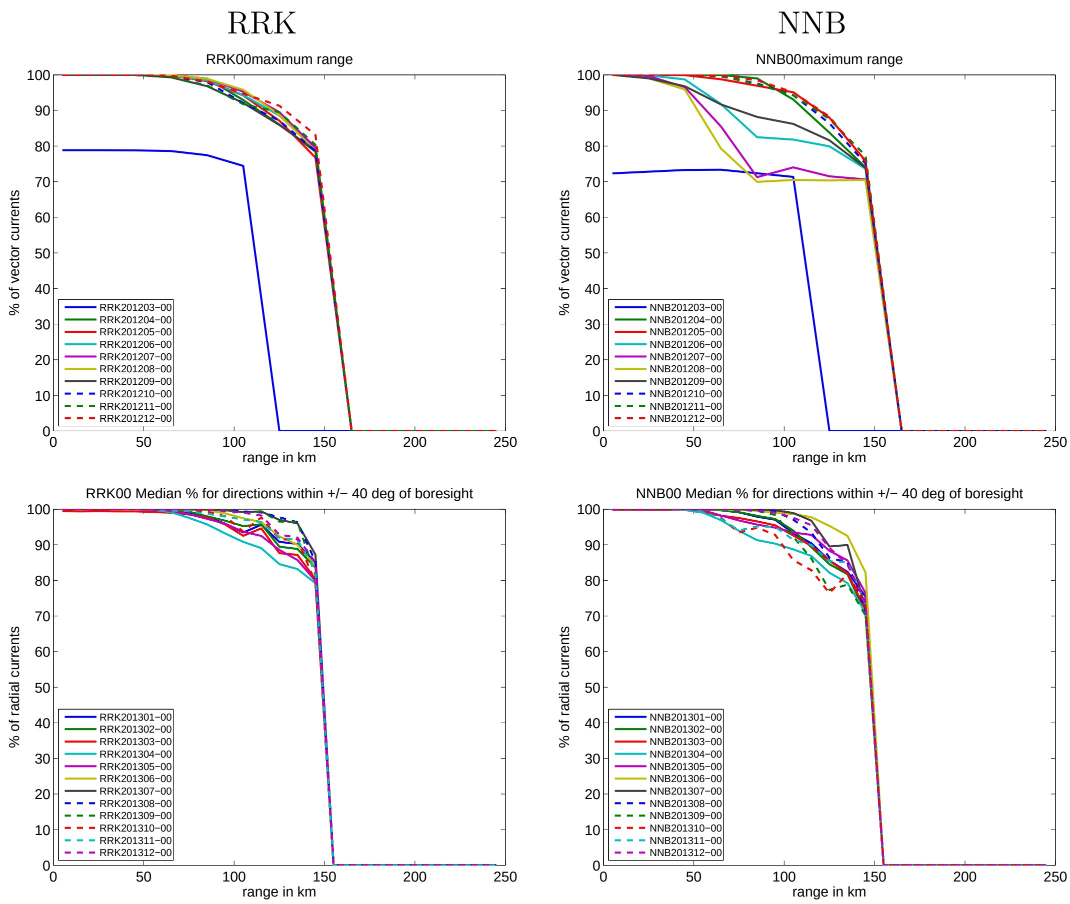

Figure 18: Radial % data return ranges 2010-2013

8 Annual mean Day-Night Returns

Figure 19 shows the median percentage vector data return for this site together with the % return broken down by time of day to show the impact of the ionosphere.

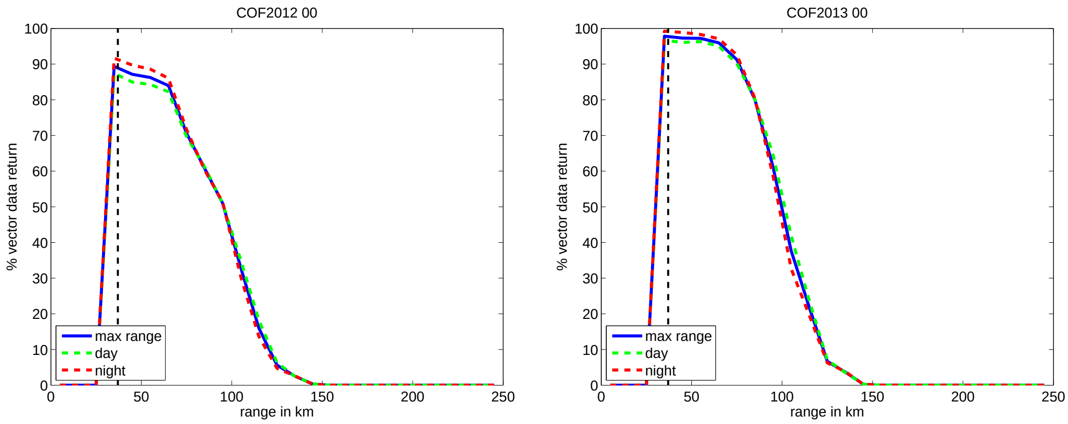

Figure 19: Vector % data return ranges 2010-2013

9 Annual mean QC and non-QC Returns

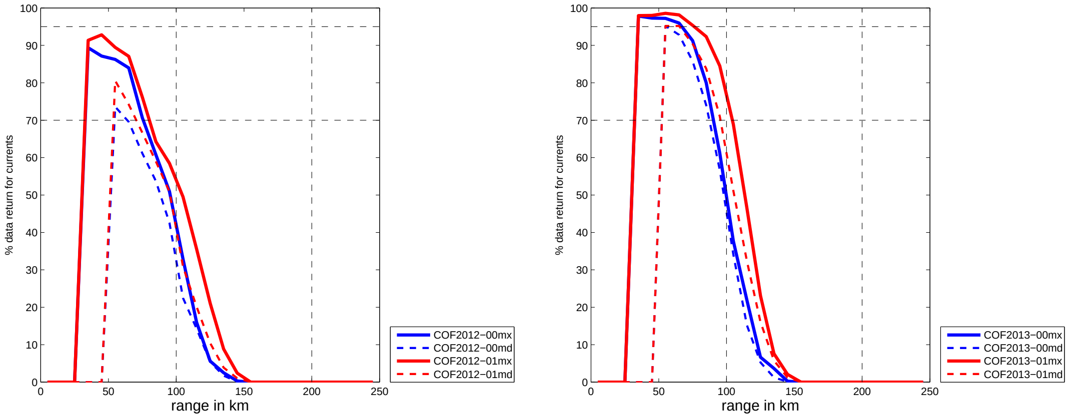

Figure 20: Comparison of QC and non-QC vector % data return ranges 2010-2013

Appendix 3: Performance of the BONC radars

In first section of this appendix the monthly performance of the BONC radar is presented. The second section shows the annual vector returns showing the average diurnal variation due to different ionospheric conditions.

10 Monthly Returns

Figure 21 shows the 50 and 90% data return ranges for each radar for the period of the deployment. Gaps in the data (connected with strainght lines in this figure) could mean there were no data or that the data are not on the IMOS server. Figure 22 shows the monthly returns for each radar for each year.

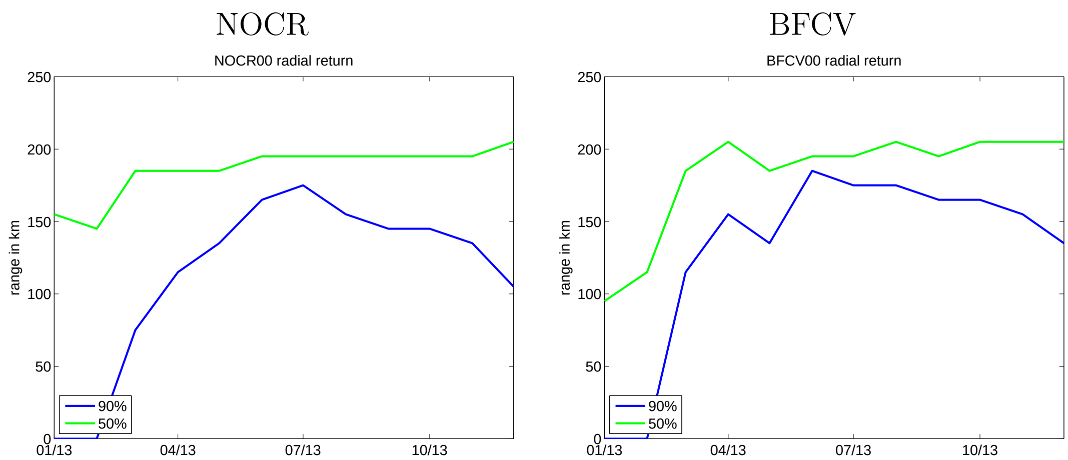

Figure 21: 50 and 90 percent data return ranges

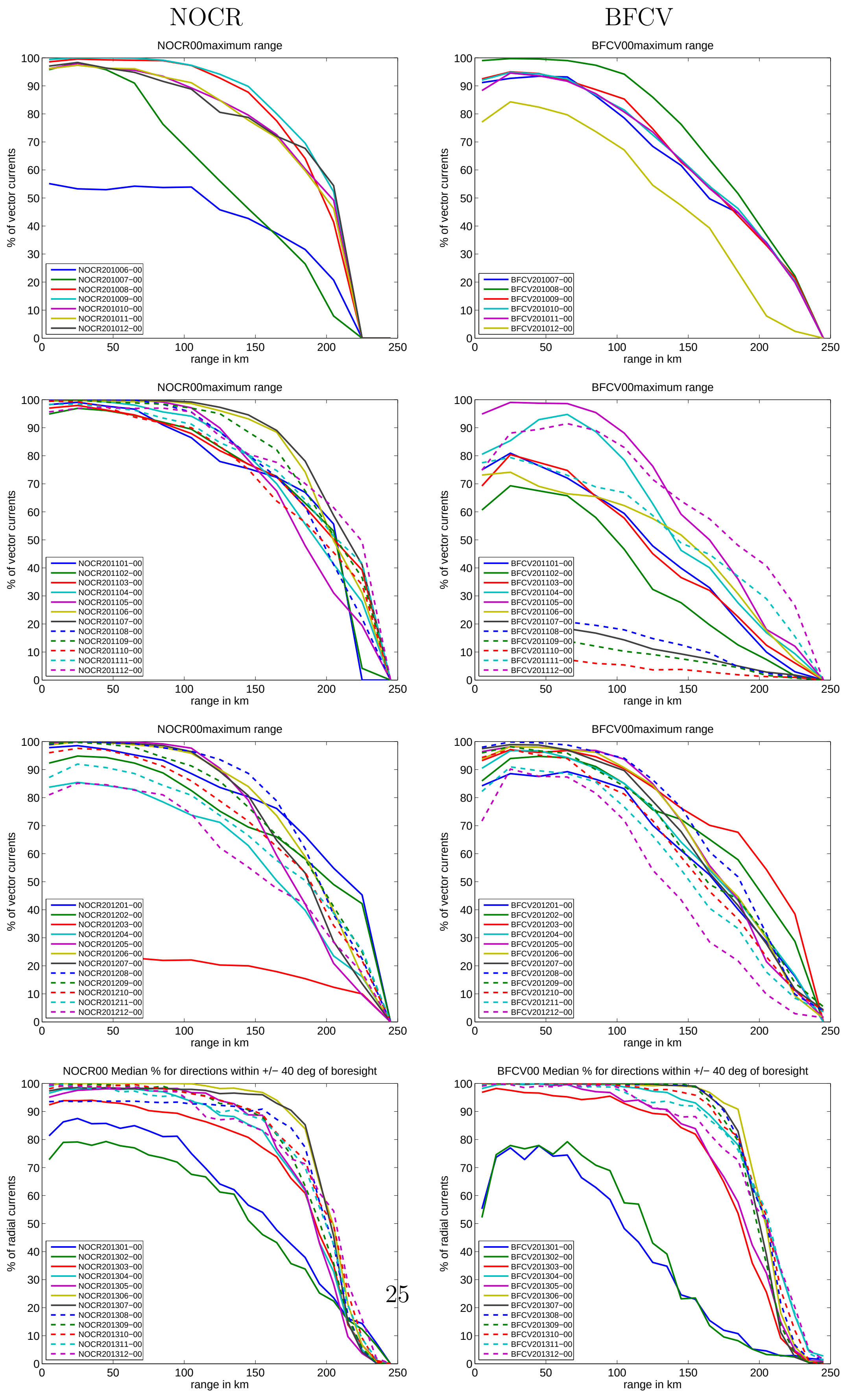

Figure 22: Radial % data return ranges 2010-2013

11 Annual mean Day-Night Returns

Figure 23 shows the median percentage vector data return for this site together with the % return broken down by time of day to show the impact of the ionosphere.

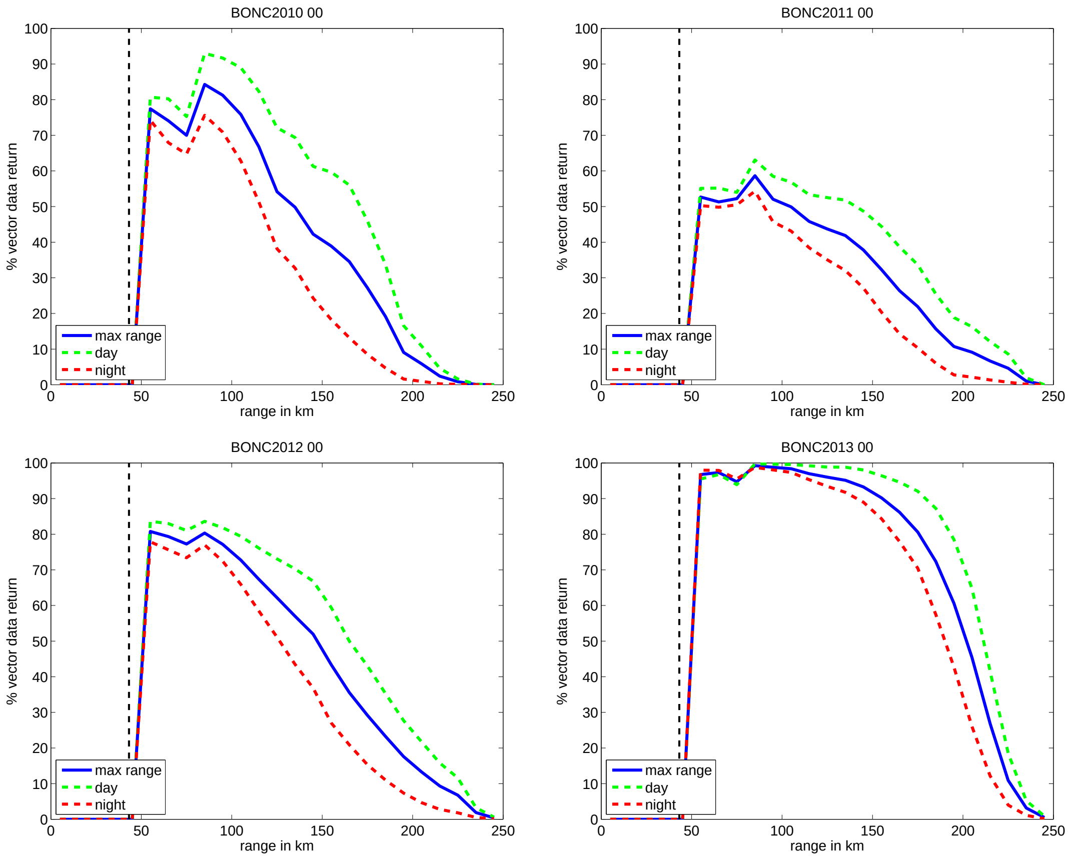

Figure 23: Vector % data return ranges 2010-2013

Appendix 4: Performance of the SAG radars

In first section of this appendix the monthly performance of the SAG radar is presented. The second section shows the annual vector returns showing the average diurnal variation due to different ionospheric conditions. The third section shows the yearly-average comparison between QC and non-QC data.

12 Monthly Returns

Figure 24 shows the 50 and 90% data return ranges for each radar for the period of the deployment. Gaps in the data (connected with strainght lines in this figure) could mean there were no data or that the data are not on the IMOS server. Figure 25 shows the monthly returns for each radar for each year.

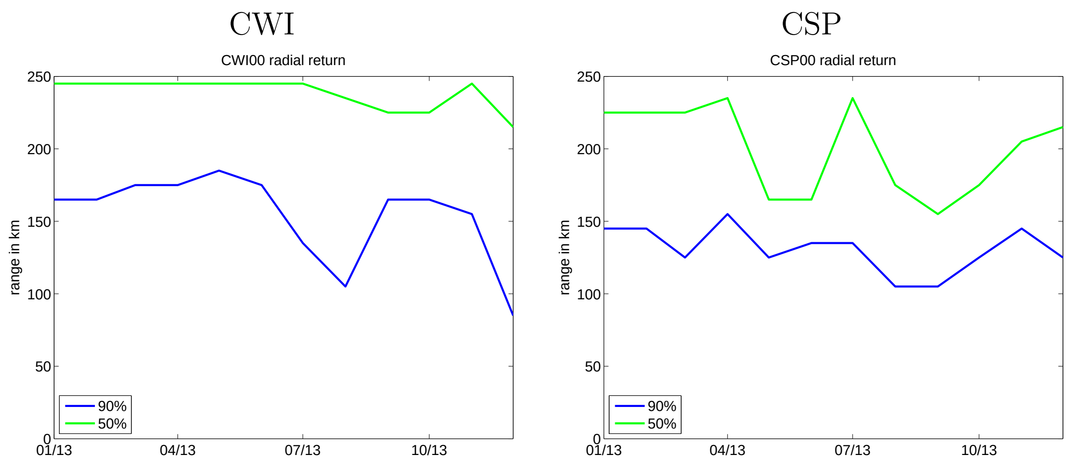

Figure 24: 50 and 90 percent data return ranges

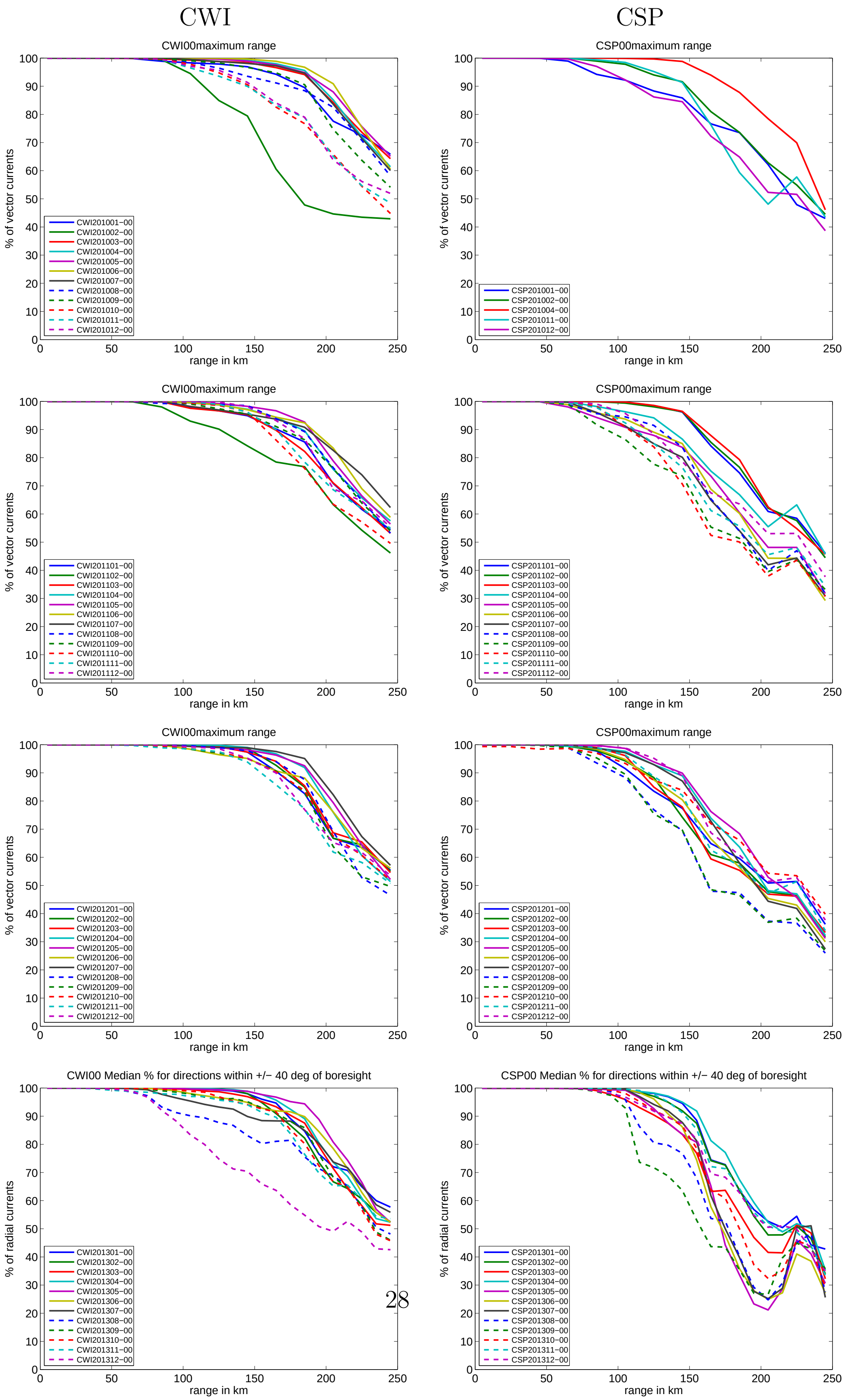

Figure 25: Radial % data return ranges 2010-2013

13 Annual mean Day-Night Returns

Figure 26 shows the median percentage vector data return for this site together with the % return broken down by time of day to show the impact of the ionosphere.

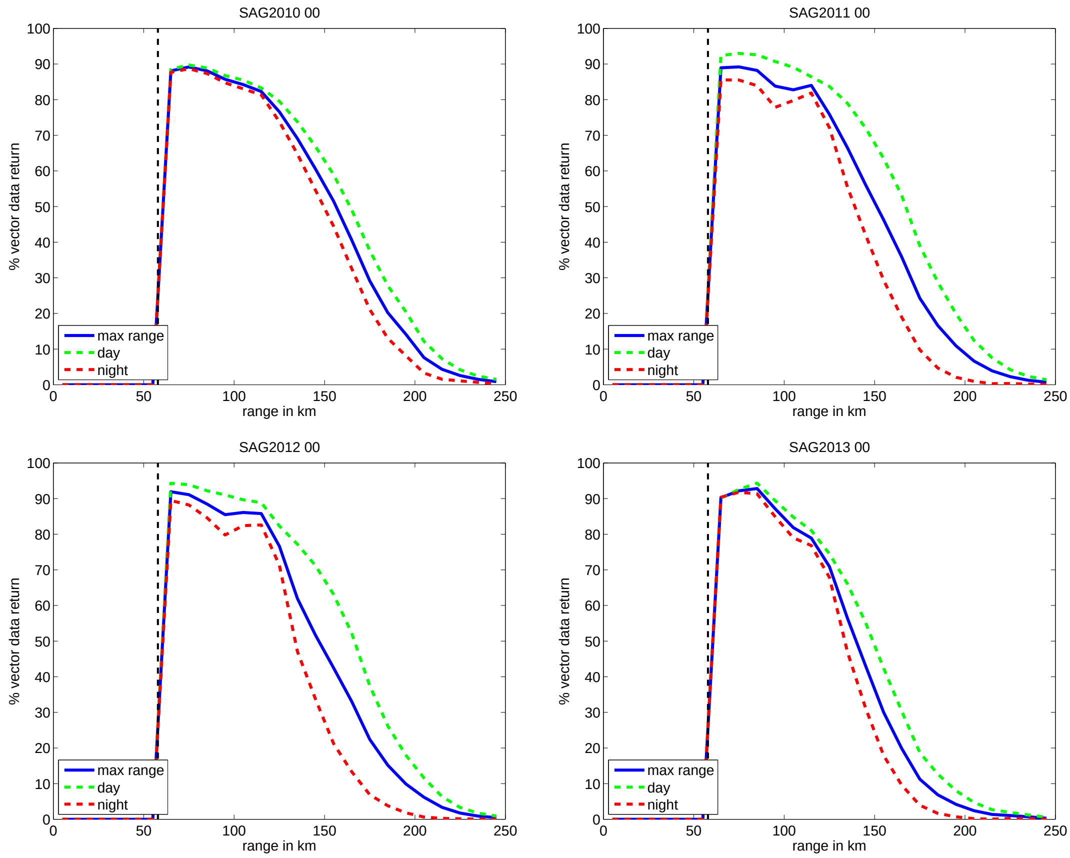

Figure 26: Vector % data return ranges 2010-2013

14 Annual mean QC and non-QC Returns

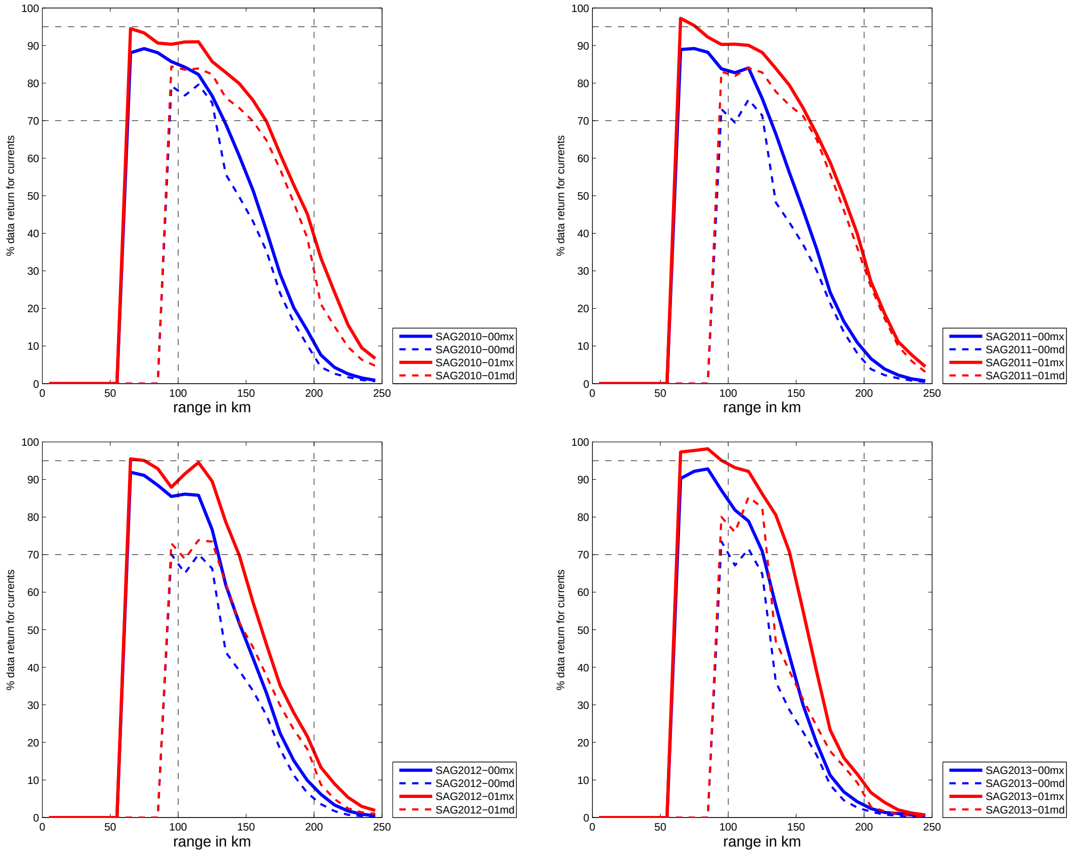

Figure 27: Comparison of QC and non-QC vector % data return ranges 2010-2013

Appendix 5: Performance of the ROT radars

In first section of this appendix the monthly performance of the ROT radar is presented. The second section shows the annual vector returns showing the average diurnal variation due to different ionospheric conditions. The third section shows the yearly-average comparison between QC and non-QC data.

15 Monthly Returns

Figure 28 shows the 50 and 90% data return ranges for each radar for the period of the deployment. Gaps in the data (connected with strainght lines in this figure) could mean there were no data or that the data are not on the IMOS server. Figure 29 shows the monthly returns for each radar for each year.

Figure 28: 50 and 90 percent data return ranges

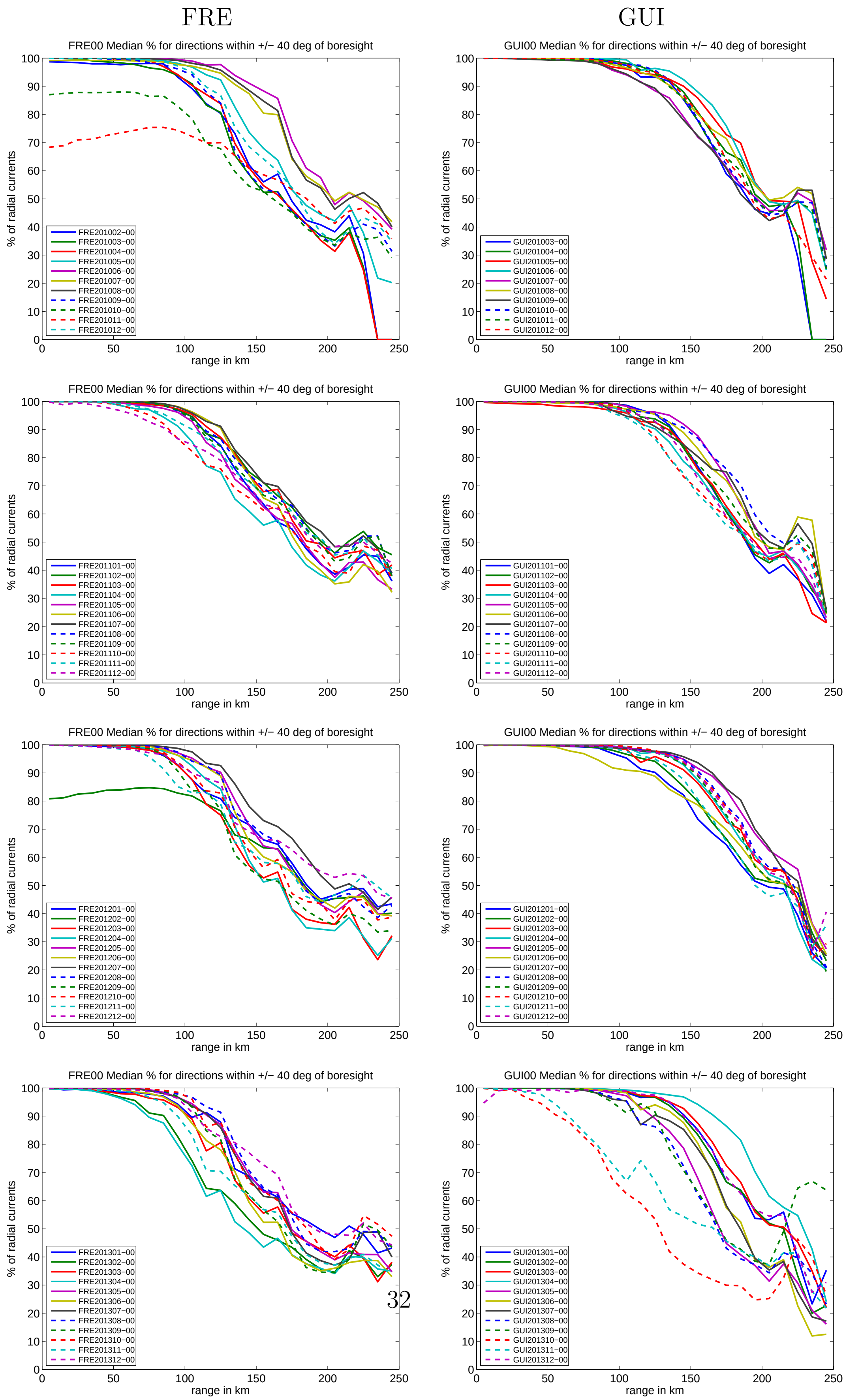

Figure 29: Radial % data return ranges 2010-2013

16 Annual mean Day-Night Returns

Figure 30 shows the median percentage vector data return for this site together with the % return broken down by time of day to show the impact of the ionosphere.

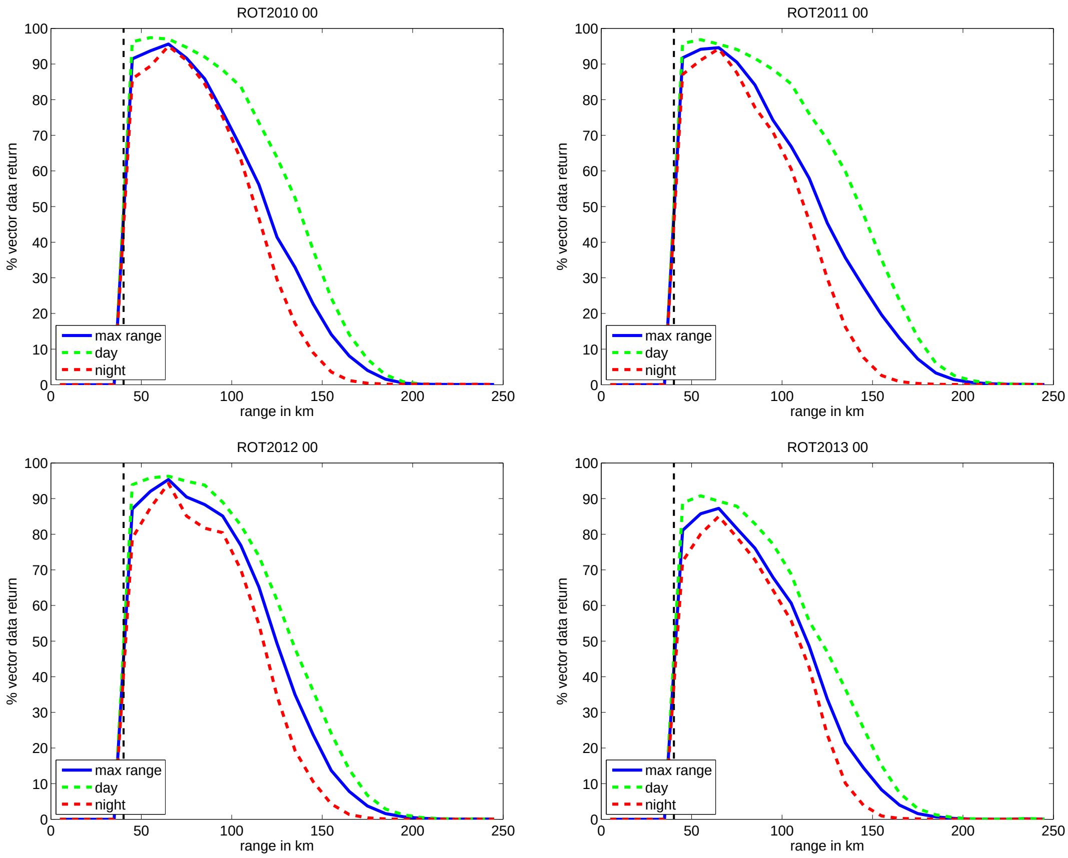

Figure 30: Vector % data return ranges 2010-2013

17 Annual mean QC and non-QC Returns

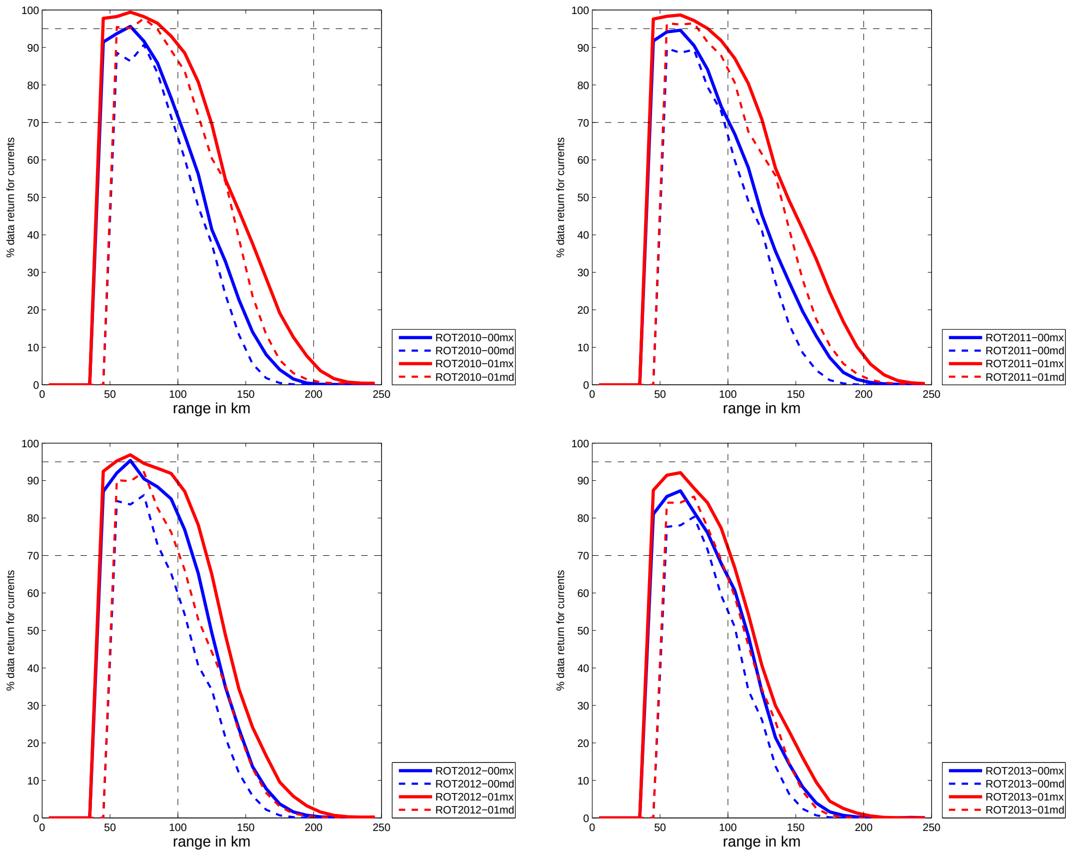

Figure 31: Comparison of QC and non-QC vector % data return ranges 2010-2013

Appendix 6: Performance of the TURQ radars

In first section of this appendix the monthly performance of the TURQ radar is presented. The second section shows the annual vector returns showing the average diurnal variation due to different ionospheric conditions.

18 Monthly Returns

Figure 32 shows the 50 and 90% data return ranges for each radar for the period of the deployment. Gaps in the data (connected with strainght lines in this figure) could mean there were no data or that the data are not on the IMOS server. Figure 33 shows the monthly returns for each radar for each year.

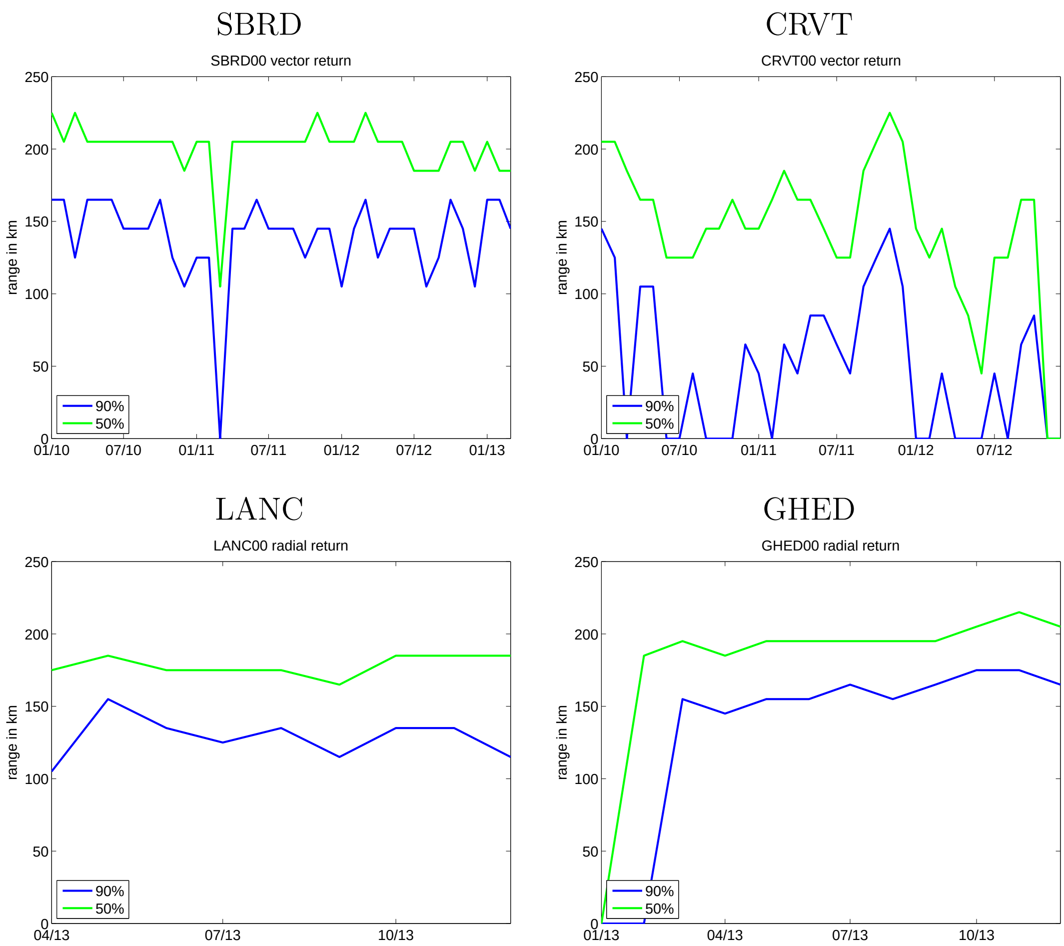

Figure 32: 50 and 90 percent data return ranges

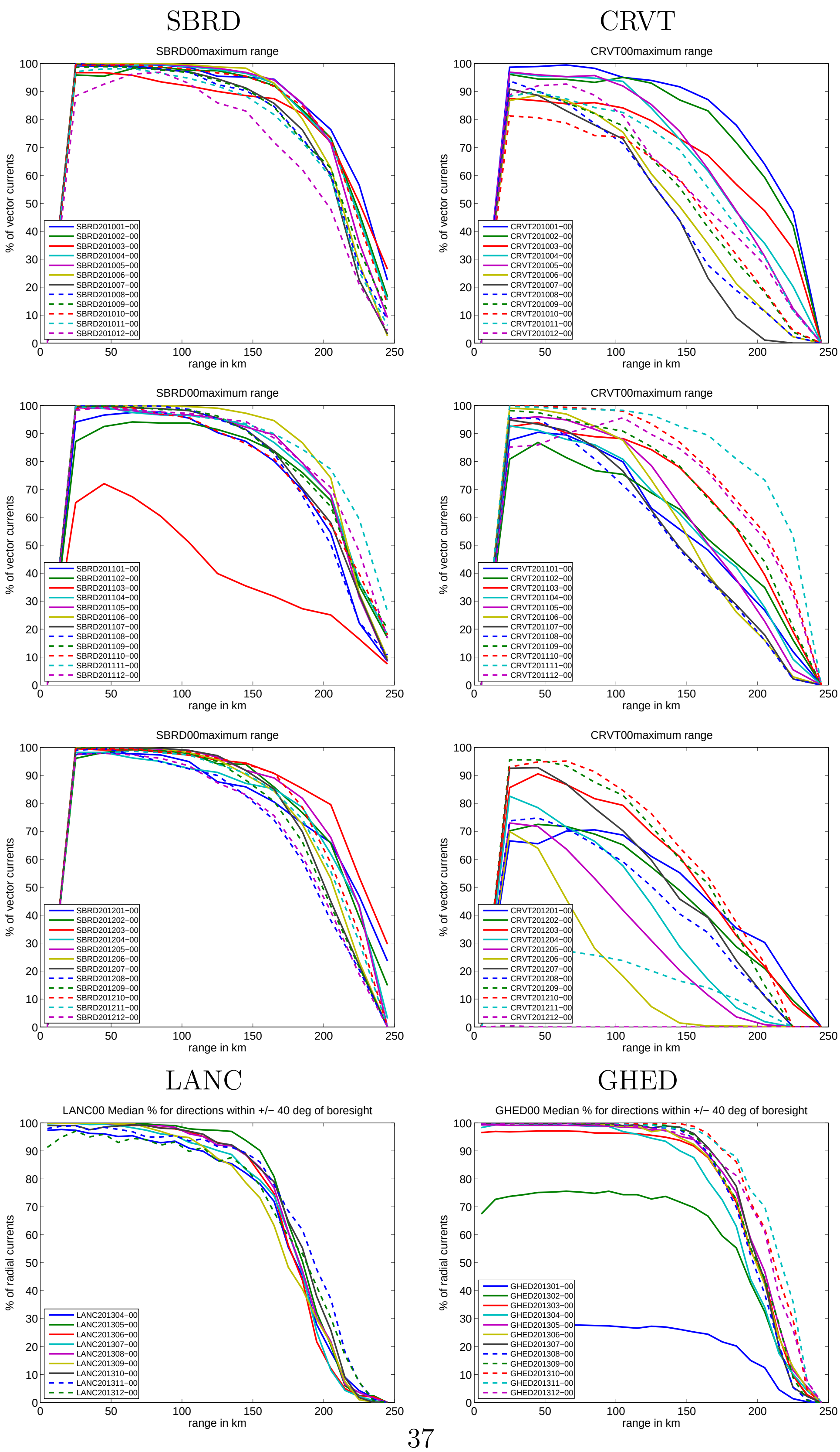

Figure 33: Radial % data return ranges 2010-2013

19 Annual mean Day-Night Returns

Figure 34 shows the median percentage vector data return for this site together with the % return broken down by time of day to show the impact of the ionosphere.

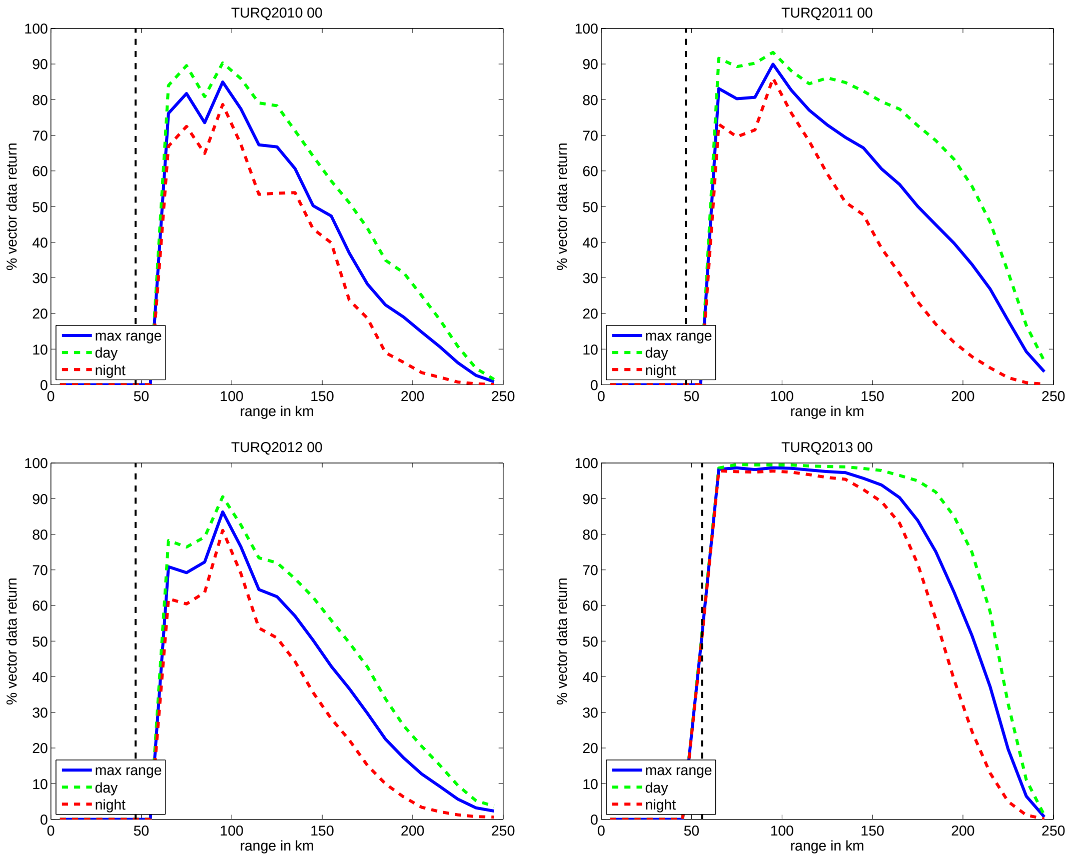

Figure 34: Vector % data return ranges 2010-2013